Supporting Information

Muñoz-Espín et al. 10.1073/pnas.1010530107

SI Text

Bacterial Strains, Phages, and Growth Conditions. *Escherichia coli* strain DH5α (Table S1), used for cloning, was grown in LB medium. When appropriate, ampicillin was added to cultures and plates at a final concentration of 100 μg/mL. *Bacillus subtilis* strains were grown at 37 °C in LB medium containing 5 mM $MgSO_4$ and supplemented with appropriate antibiotics: kanamycin (5 μg/mL), erythromycin (1 μg/mL), and/or spectinomycin (100 μg/mL). *B. subtilis mreB* mutant strains (Table S1) can be propagated with near wild-type growth rate and cell morphology in growth medium supplemented with high concentrations of magnesium (1). Thus, when cytoskeleton mutants were used, $MgSO_4$ concentrations were increased to 25 mM in all cultures.

Generally, overnight cultures were diluted 1:50 in fresh medium and incubated for 2–3 h to reestablish exponential growth before manipulation. Expression of YFP fusions was induced by addition of 0.5% xylose at the time of phage infection. To express CFP fusions under a hyper-spank promoter, the culture media were supplemented with 1 mM isopropyl-β-D-thiogalactopyranoside (IPTG) at the time of infection.

Phage plaque assays were done by standard methods (2).

Plasmid Construction. The *yfp* fusion of ϕ29 gene *3*, encoding the terminal protein (TP), was constructed as follows. Gene *3* was amplified by PCR from ϕ29 DNA using primer sets YFP-TP_U and YFP-TP_L (Table S3). The PCR product obtained was digested with XhoI/EcoRI and cloned into the *B. subtilis amyE* integration vector pSG5472 (3) digested with the same enzymes. As a result, gene *3* fused in frame to the *yfpmut2* gene at its C terminus (pSGDM5) was located behind the xylose-inducible promoter P_{xyl}. pSGDM5 was used to transform competent *B. subtilis* cells. Spectinomycin-resistant transformants were tested for their ability to degrade starch to select for double-crossover transformants. To generate construct pDP150-TP, a PCR product containing gene *3* was amplified from the ϕ29 genome by using primers TP_1 and TP_2. This fragment was digested with restriction enzymes NheI and SphI and cloned into equivalent sites of the *thrC*-integrating vector pDP150 (4), which contains the IPTG-inducible $P_{hyper\text{-}spank}$ promoter. To generate plasmid pDP150-CFP, a PCR product containing the *cfp(Bs)* gene and a *B. subtilis* ribosome-entry site was amplified from plasmid pDR200 (5) by using primers CFP(BS)_U and CFP(BS)_L. This fragment was digested with restriction enzymes HindIII and NheI and cloned into equivalent sites of the *thrC*-integrating vector pDP150 (4). Plasmid pDP150-CFP-2 was generated by using the QuikChange site directed-mutagenesis kit (Stratagene) and primers 150-SpeI-1 and 150-SpeI-2 to introduce a *Spe*I restriction site at the multiple cloning site (MCS) of the vector. To generate constructs pDP150-CFP/TP, pDP150-CFP/TP N-terminal (TP-Nt), pDP150-CFP/TP N-terminal/intermediate (TP-NtI), pDP150-CFP/intermediate TP (TP-I), pDP150-CFP/intermediate/C-terminal TP (TP-ΔNt), and pDP150-CFP/C-terminal TP (TP-Ct), specific regions of the ϕ29 gene *3* were amplified using the following primer sets: TP_U and TP_L, TP_U and TP-Nt_L, TP_U and TP-NtI_L, TP-I_U and TP-I_L, TP-I_U and TP_L and TP-Ct_U and TP_L, respectively. Each PCR product was digested with SphI and SpeI and cloned independently into the SphI and SpeI sites of plasmid pDP150-CFP-2. The plasmids obtained were used to transform competent *B. subtilis* cells, and erythromycin-resistant double-crossover transformants were selected by the loss of spectinomycin tolerance. To construct plasmid pET-TP/NtI, the DNA sequence of ϕ29 gene *3* spanning nucleotides 1–519 was amplified with primers TP-NcoI-U and TP-NtI-NotI-L. The PCR product obtained was digested with NcoI and NotI and cloned into the expression plasmid pET-28b(+) (Novagen) digested with the same enzymes. Likewise, plasmids pET-TP/Nt, pET-TP/ΔNt, and pET-TP/Ct were constructed using the following primer sets to amplify the desired regions of gene *3*: TP-NdeI_U and TP-Nt-NotI_L, TP-I-NdeI_U and TP-BamHI_L, and TP-Ct-NdeI_U and TP-BamHI_L, respectively. Such a DNA fragment contains a 5′ NdeI site and a stop codon followed by a NotI or a BamHI site at the 3′ end, as indicated by the primer name. These DNA fragments were digested with the corresponding restriction enzymes and cloned into plasmid pET-28b(+) digested with the same enzymes. To generate construct pDP150-CFP/TP8-PRD1, the PRD1 gene *VIII* was amplified using primers TP8-R and TP8-L. The PCR product was digested with SphI and SpeI and cloned into the SphI and SpeI sites of plasmid pDP150-CFP-2.

Protein Treatment with Thrombin. Proteins containing histidine tags were digested with thrombin using the thrombin cleavage capture kit (Novagen). Complete cleavage of TP mutants was confirmed by Tris-Tricine-SDS electrophoresis. The biotinylated thrombin used to cleave these mutants then was removed from the sample by using the streptavidin-agarose column provided with the kit. Finally, the samples containing the purified proteins were dialyzed against 50 mM Tris-HCl (pH 7.5) containing 7 mM 2-mercaptoethanol, 1 mM EDTA, 200 mM NaCl, and 50% glycerol.

Immunofluorescence Microscopy. Blocking buffer contained 0.5% (wt/vol) casein (Sigma). Affinity-purified rat polyclonal antibodies against p3 were used at 1:1,000 dilution, and incubations were carried out for 1 h at room temperature. Polyclonal antibodies were centrifuged for 10 min at 14,000 × *g* at 4 °C before use to precipitate possible antibody aggregates. All samples were mounted for epifluorescence microscopy in multispot microscope slides (C.A. Hendley, Essex, Ltd) and supplemented with 0.2 μg/mL DAPI or with 1.34 μg/mL TO-PRO-3, when required.

Image Acquisition and Image Analysis. Imaging acquisition was performed as described (6) using a Sony CoolSnap HQ cooled charge-coupled device camera (Roper Scientific) attached to a Zeiss Axiovert 200M microscope. The digital images were acquired and analyzed with MetaMorph version 6 software. Images of fluorescent samples were deconvolved within MetaMorph and assembled in Adobe Photoshop version 7. Image manipulation was kept to a minimum. For general purposes, images were scaled and then saved as eight-bit images.

Analysis of Viral DNA by Gel Electrophoresis. Synthesis of viral DNA in vivo was analyzed as described (7). Basically, total intracellular DNA was isolated at different times after infection and analyzed in 0.6% agarose gels.

Real-Time PCR. The primer sets R-OUT-SUPER and R-25 were used to amplify regions of the genome of phage ϕ29 (Table S3). The data obtained for samples were interpolated to standard curves constructed with known amounts of phage DNA. The results are expressed as nanograms of DNA per milliliter of culture.

Yeast Two-Hybrid Experiments. *B. subtilis* ORFs including the *hbs*, *noc*, *smc*, *scpA*, and *scpB* genes and ϕ29 genes *2* and *3* were amplified by PCR from strain 168 and ϕ29 genomic DNA, respectively. The DNA fragments were cloned into the pGBDU bait vector (Ura^+) and the pGAD prey vector (Leu^+), fused to the C

terminus of the GAL4 DNA-binding domain (BD) and the GAL4 activation domain (AD), respectively. The haploid strain PJ69-4a of *Saccharomyces cerevisiae* was transformed by different combinations of bait vectors. Ura^+ colonies were mated with haploid PJ69-4α strains containing various prey vectors, and diploids (Ura^+ Leu^+) were selected on synthetic complete medium lacking leucine and uracil. The diploid cells were tested for expression of the interaction phenotypes (His^+ and Ade^+) by replica-plating the diploids onto selective plates lacking histidine or adenine, as described previously (8). Interaction phenotypes were scored after incubation for 7 d at 30 °C. Specific interactions were shown to be reproducible and not associated with self-activation.

1. Formstone A, Errington J (2005) A magnesium-dependent *mreB* null mutant: Implications for the role of *mreB* in *Bacillus subtilis*. *Mol Microbiol* 55:1646–1657.
2. Sambrook J, Fritsch EF, Maniatis T (1989) *Molecular Cloning: A Laboratory Manual* (Cold Spring Harbor Lab Press, Cold Spring Harbor, NY).
3. Lemon KP, Grossman AD (2000) Movement of replicating DNA through a stationary replisome. *Mol Cell* 6:1321–1330.
4. Kearns DB, Losick R (2005) Cell population heterogeneity during growth of *Bacillus subtilis*. *Genes Dev* 19:3083–3094.
5. Doan T, Marquis KA, Rudner DZ (2005) Subcellular localization of a sporulation membrane protein is achieved through a network of interactions along and across the septum. *Mol Microbiol* 55:1767–1781.
6. Muñoz-Espín D, et al. (2009) The actin-like MreB cytoskeleton organizes viral DNA replication in bacteria. *Proc Natl Acad Sci USA* 106:13347–13352.
7. Bravo A, Hermoso JM, Salas M (1994) A genetic approach to the identification of functional amino acids in protein p6 of *Bacillus subtilis* phage ϕ29. *Mol Gen Genet* 245:529–536.
8. Carballido-López R, et al. (2006) Actin homolog MreBH governs cell morphogenesis by localization of the cell wall hydrolase LytE. *Dev Cell* 11:399–409.

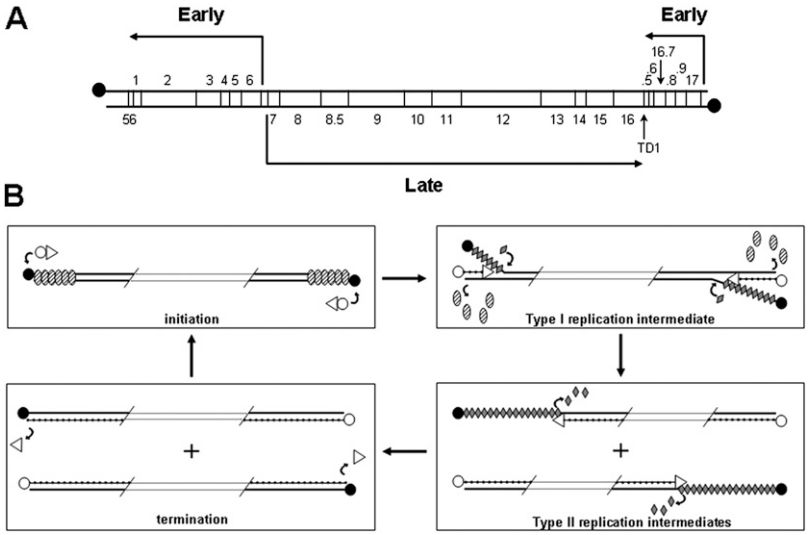

Fig. S1. Genetic and transcriptional map of the ϕ29 genome and mechanism of in vitro ϕ29 DNA replication. (*A*) Map of the ϕ29 genome. The direction of transcription and length of the transcripts are indicated by arrows, and the positions of genes are indicated by numbers. TD1 corresponds to the bidirectional transcriptional terminator located between the convergently transcribed late and right-side early operons. Black circles represent the TP covalently linked to the 5′ DNA ends. (*B*) Overview of the in vitro ϕ29 DNA replication mechanism. Replication starts by recognition of the p6-nucleoprotein complexed origins of replication by a TP/DNA polymerase heterodimer. The DNA polymerase then catalyses the addition of the first deoxyAMP to the TP present in the heterodimer complex. After a transitional step, these two proteins dissociate, and the DNA polymerase continues processive elongation until replication of the nascent DNA strand is completed. Replication is coupled to strand displacement. The ϕ29-encoded SSB protein p5 binds to the displaced ssDNA strands and is removed by the DNA polymerase during later stages of the replication process. Continuous polymerization results in the generation of two fully replicated ϕ29 genomes. Circles, TP; triangles, DNA polymerase; ovals, replication initiator protein p6; diamonds, SSB protein p5; de novo synthesized DNA is shown as beads on a string. Adapted from ref. 1.

1. Muñoz-Espín D, et al. (2009) The actin-like MreB cytoskeleton organizes viral DNA replication in bacteria. *Proc Natl Acad Sci USA* 106:13347–13352.

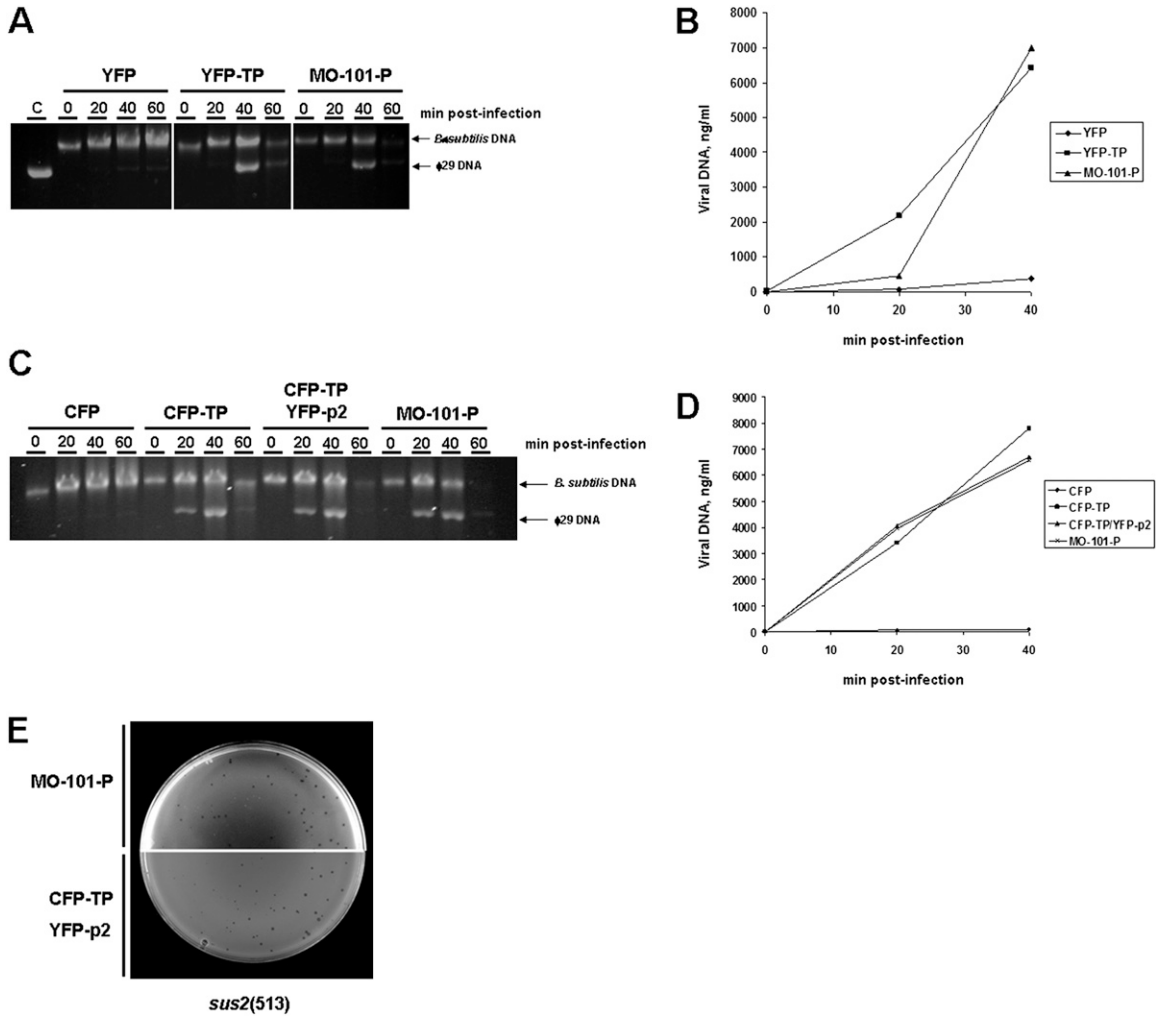

Fig. S2. ϕ29 TP fluorescent fusions are functional in vivo. (*A* and *B*) Complementation experiments using a *sus3*(91) mutant phage and *B. subtilis* strains DM-022 (expressing YFP), DM-021 (expressing YFP-TP), and MO-101-P [suppressing the nonsense mutation of *sus3*(91) mutant phage]. (*A*) Agarose gel electrophoresis analysis illustrating the amount of viral DNA accumulated by the *B. subtilis* strain DM-021. Xylose-induced cells were infected with a *sus3*(91) mutant phage at a multiplicity of infection (MOI) of 5, and aliquots were harvested and processed at the indicated times postinfection. Location of the ϕ29 genome and *B. subtilis* chromosomal DNA is indicated. (*B*) ϕ29 intracellular accumulated DNA was quantified by real-time PCR after infection at an MOI of 5 at the indicated times postinfection. Phage DNA production was expressed as nanograms of viral DNA per milliliter of culture. The amount of intracellular phage ϕ29 DNA accumulated was analyzed by agarose gel electrophoresis (*C*) and real-time PCR (*D*) after infection of the following *B. subtilis* strains with a *sus3*(91) mutant phage: DM-024 (expressing CFP), DM-025 (expressing CFP-TP), DM-023 (expressing CFP-TP and YFP-p2), and MO-101-P (suppressor strain). IPTG- and/or xylose-induced cells were infected at an MOI of 5, harvested at the indicated times after infection, and processed as described in *Materials and Methods*. Locations of the ϕ29 genome and *B. subtilis* chromosomal DNA are indicated. The amounts of accumulated phage DNA (nanograms of viral DNA per milliliter of culture) are expressed in the graph as a function of time after infection. (*E*) Exponentially growing *B. subtilis* cells of strain DM-023 (expressing CFP-TP and YFP-p2) were infected with ϕ29 mutant phage *sus2*(513) containing a suppressible stop codon in the DNA polymerase-encoding gene *2* (1). Next, samples were mixed with liquid top agar containing 0.5% xylose, spread on LB agar plates, and incubated overnight at 37 °C. Plaque formation similar to that of strain DM-023 was observed when *sus2*(513) phages were used to infect the suppressor strain MO-101-P, indicating that the YFP-p2 inducible fusion is functional.

1. Moreno F, Camacho A, Viñuela E, Salas M (1974) Suppressor-sensitive mutants and genetic map of *Bacillus subtilis* bacteriophage ϕ29. *Virology* 62:1–16.

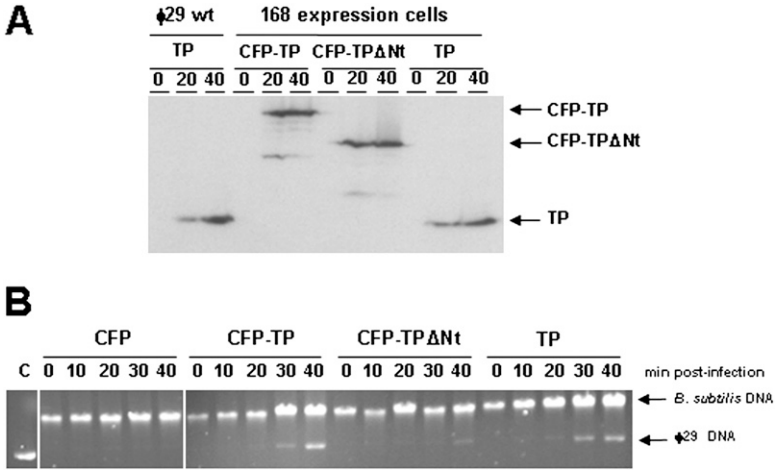

Fig. S3. The N-terminal domain of the TP is important for efficient ϕ29 DNA replication. DM-024 (expressing CFP), DM-025 (expressing CFP-TP), DM-029 (expressing CFP-TPΔNt), and DM-032 (expressing wild-type TP) cells were grown at 37 °C in LB medium supplemented with 2% glucose to an OD_{600} of 0.4. Cells then were infected with a *sus3*(91) mutant phage at an MOI of 1, and IPTG was added to a final concentration of 1 mM. At the indicated times (minutes), cell samples were harvested, processed, and subjected to SDS/PAGE and Western blotting (*A*) or agarose gel electrophoresis (*B*) (*SI Text*). (*A*) As an internal control, *B. subtilis* 168 cells were infected with ϕ29 wild-type phage, and the production of TP was analyzed at the indicated times postinfection. Arrows indicate positioning of CFP-TP, CFP-TPΔNt, and TP bands. (*B*) Location of the ϕ29 genome and *B. subtilis* chromosomal DNA.

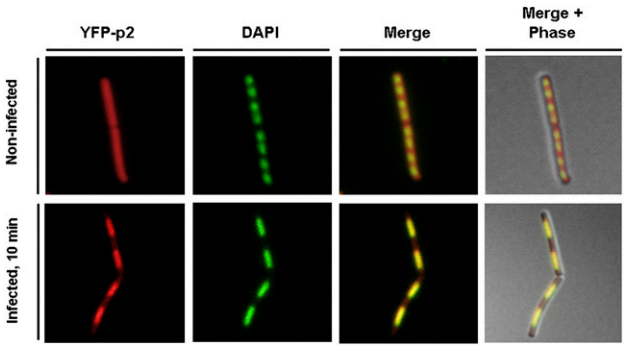

Fig. S4. YFP-p2 colocalizes with the bacterial nucleoid at early infection times. YFP, DAPI staining, and merged images of *B. subtilis* cells expressing xylose-induced YFP-p2 (strain DM-020). Cells were grown to midexponential phase in LB medium supplemented with 2% glucose at 37 °C, and at an OD_{600} of 0.4 the culture was supplemented with 0.5% xylose. Subsequently, the culture was divided, and half the culture was infected with a *sus2*(513) mutant phage at an MOI of 5. Samples were harvested 10 min after xylose addition (or 10 min after infection) and analyzed by fluorescence microscopy techniques (*Materials and Methods* and *SI Text*). For clarity, YFP fluorescent signals and DAPI staining are false-colored red and green, respectively.

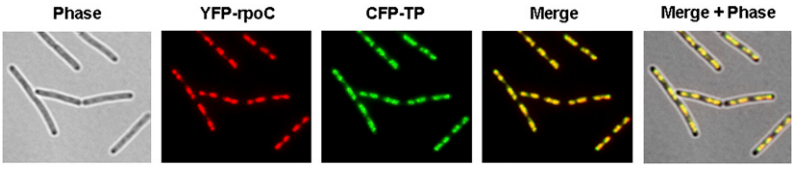

Fig. S5. *B. subtilis* RNA polymerase β′ subunit and ϕ29 TP colocalize at the bacterial nucleoid. Phase-contrast, CFP, YFP, and merged images of typical cells (*B. subtilis* strain DM-033) simultaneously expressing IPTG-induced CFP-TP and xylose-induced YFP-rpoC fusion proteins. Cultures were grown at 37 °C in LB medium supplemented with 2% glucose. At an OD_{600} of 0.4, cultures were additionally supplemented with 0.5% xylose and 1 mM IPTG. Samples were harvested and processed for fluorescence microscopy 30 min after the addition of the inductors. For clarity, YFP and CFP fluorescent signals are false-colored red and green, respectively.

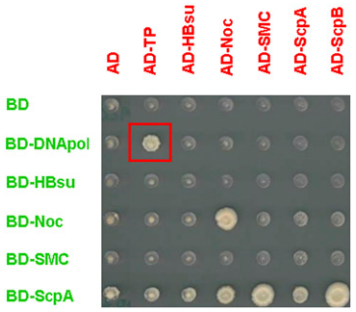

Fig. S6. ϕ29 TP does not interact with nucleoid-associated proteins of *B. subtilis*. ϕ29 TP protein as GAL4-AD fusion was tested for interaction with full-length HBsu, Noc, SMC, and ScpA as baits (GAL4-BD fusions). No evidence of specific interaction/s was obtained. Interactions of ϕ29 TP-DNA polymerase (red square), Noc-Noc, SMC-ScpA, ScpA-ScpA, and ScpA-ScpB were obtained as internal controls. The BD-TP fusion was not functional in yeast and thus has not been included in this assay. Auto-interaction was tested by crossing preys and baits with the BD and AD expressed from empty vectors. The BD-ScpB fusion resulted in self-activation and has not been included. The yeast two-hybrid assay was performed in duplicate with independent yeast clones.

Table S1. Strains used

Strain	Relevant genotype	Construction, source, or reference
E. coli		
DH5 α	ϕ80d*lac*ZΔM15, *rec*A1, *end*A1, *gyr*AB, *thi*-1, *hsd*R17(r_K^-, m_K^+), *sup*E44, *rel*A1, *deo*R, Δ(*lacZYA-arg*F) U169, *pho*A	Laboratory stock
XL1 blue	*rec*A1, *end*A1, *gyr*A96, *thi*-1, *hsd*R17(r_K^-, m_K^+), *sup*E44, *rel*A1, *lac*, [F′, *proAB*, *lac*I^qZΔM15::Tn10(tet^r)]	Laboratory stock
BL21(DE3)	F^-, *omp*T, *hsd*S_B(r_B-, m_B-), *dcm*, *gal*, λ(DE3)	Laboratory stock
DM-049	XL1 blue containing plasmid pDP150-CFP	pDP150-CFP → XL1 blue (Amp)
DM-050	XL1 blue containing plasmid pDP150-CFP/TP	pDP150-CFP/TP → XL1 blue (Amp)
DM-051	XL1 blue containing plasmid pDP150-CFP/TP-PRD1	pDP150-CFP/TP8-PRD1 → XL1 blue (Amp)
B. subtilis		
110NA	*trpC2 spo0A3 su*$^-$	Moreno et al. (1)
168	*trpC2,* considered *wild-type* strain	*Bacillus* Genetic Stock Center
MO-101-P	*thr*$^-$ *spo0A*$^-$ *su*$^+$	Mellado et al. (2)
SWV215	*trpC2 pheA1 Ω(spo0A::kan)*	Xu and Strauch (3)
DM-020	*trpC2 Ω(amyE::*P_{xyl}*-yfp-p2 spc)*	pSGDM3 → 168 (Sp)
DM-021	*trpC2 Ω(amyE::*P_{xyl}*-yfp-p3 spc)*	pSGDM4 → 168 (Sp)
DM-022	*trpC2 Ω(amyE::*P_{xyl}*-yfp spc)*	pSG5472 → 168 (Sp)
DM-023	*trpC2 Ω(amyE::*P_{xyl}*-yfp-p2 spc) Ω(thrC::*$P_{hiper\text{-}spank}$*-cfp-p3 erm)*	pSGDM3, pDP150-CFP → 168 (Sp)
DM-024	*trpC2 Ω(thrC::*$P_{hiper\text{-}spank}$*-cfp erm)*	pDP150-CFP → 168 (Erm)
DM-025	*trpC2 Ω(thrC::*$P_{hiper\text{-}spank}$*-cfp-p3 erm)*	pDP150-CFP/TP → 168 (Erm)
DM-026	*trpC2 Ω(thrC::*$P_{hiper\text{-}spank}$*-cfp-p3Nt erm)*	pDP150-CFP/TP-Nt → 168 (Erm)
DM-027	*trpC2 Ω(thrC::*$P_{hiper\text{-}spank}$*-cfp-p3NtI erm)*	pDP150-CFP/TP-NtI → 168 (Erm)
DM-028	*trpC2 Ω(thrC::*$P_{hiper\text{-}spank}$*-cfp-p3I erm)*	pDP150-CFP/TP-I → 168 (Erm)
DM-029	*trpC2 Ω(thrC::*$P_{hiper\text{-}spank}$*-cfp-p3ΔNt erm)*	pDP150-CFP/TP-ΔNt → 168 (Erm)
DM-030	*trpC2 Ω(thrC::*$P_{hiper\text{-}spank}$*-cfp-p3Ct erm)*	pDP150-CFP/TP-Ct → 168 (Erm)
3725	*trpC2 Ω(neo3427)ΔmreB*	Formstone et al. (4)
DM-031	*trpC2 Ω(amyE::*P_{xyl}*-yfp-p3 spc) Ω(neo3427)ΔmreB*	3725 → DM-021 (Erm)
DM-032	*trpC2 Ω(thrC::*$P_{hiper\text{-}spank}$*-gene 3 erm)*	pDP150-TP → 168 (Erm)
BS126	*trpC2 Ω(rpoC::rpoC-yfp kan)*	Davies et al. (5)
DM-033	*trpC2 Ω(thrC::*$P_{hiper\text{-}spank}$*-cfp-p3 erm) Ω(rpoC::rpoC-yfp kan)*	pDP150-CFP/TP → BS126 (Erm)
DM-060	*trpC2 Ω(thrC::*$P_{hiper\text{-}spank}$*-cfp-VIII* PRD1 *erm)*	pDP150-CFP/TP8-PRD1→ 168 (Sp)
S. cerevisiae		
PJ69–4a	*MATa trpl-901 leu2-3,112 ura3-52 his3-200 gal4Δ gal80Δ LYS2::GAL1-HIS3 GAL2-ADE2met2::GAL7-lacZ*	James et al. (6)
PJ69–4α	*MATα trpl-901 leu2-3,112 ura3-52 his3-200 gal4Δ gal80Δ LYS2::GAL1-HIS3 GAL2-ADE2met2::GAL7-lacZ*	Noirot-Gros et al. (7)
yNG132	PJ69–4α, pGAD	Noirot-Gros et al. (7)
yNG3811	PJ69–4α, pGAD::*p3*	This work
yNG1928	PJ69–4α, pGAD::*smc*	Dervyn et al. (8)
yNG64	PJ69–4α, pGAD::*scpA*	Dervyn et al. (8)
yNG66	PJ69–4α, pGAD::*scpB*	Dervyn et al. (8)
yNG121	PJ69–4a, pGBDU	Noirot-Gros et al. (7)
yNG3809	PJ69–4a, pGBDU::*p2*	This work
yNG129	PJ69–4a, pGBDU::*smc*	Dervyn et al. (8)
yNG74	PJ69–4a, pGBDU::*scpA*	Dervyn et al. (8)

Antibiotic resistance gene abbreviations are as follows: *erm*, erythromycin; *kan*, kanamycin; *neo*, neomycin; *spc*, spectinomycin. "X" → "Y" indicates that strain Y was transformed with DNA from source X, with selected marker in parentheses. Amp, ampicillin; Em, erythromycin; Sp, spectinomycin.

1. Moreno F, Camacho A, Viñuela E, Salas M (1974) Suppressor-sensitive mutants and genetic map of *Bacillus subtilis* bacteriophage ϕ29. *Virology* 62:1–16.
2. Mellado RP, Viñuela E, Salas M (1976) Isolation of a strong suppressor of nonsense mutations in *Bacillus subtilis*. *Eur J Biochem* 65:213–223.
3. Xu K, Strauch MA (1996) Identification, sequence, and expression of the gene encoding gamma-glutamyltranspeptidase in *Bacillus subtilis*. *J Bacteriol* 178:4319–4322.
4. Formstone A, Errington J (2005) A magnesium-dependent *mreB* null mutant: Implications for the role of *mreB* in *Bacillus subtilis*. *Mol Microbiol* 55:1646–1657.
5. Davies KM, Dedman AJ, van Horck S, Lewis PJ (2005) The NusA:RNA polymerase ratio is increased at sites of rRNA synthesis in *Bacillus subtilis*. *Mol Microbiol* 57:366–379.
6. James P, Halladay J, Craig EA (1996) Genomic libraries and a host strain designed for highly efficient two-hybrid selection in yeast. *Genetics* 144:1425–1436.
7. Noirot-Gros MF, et al. (2002) An expanded view of bacterial DNA replication. *Proc Natl Acad Sci USA* 99:8342–8347.
8. Dervyn E, et al. (2004) The bacterial condensin/cohesin-like protein complex acts in DNA repair and regulation of gene expression. *Mol Microbiol* 51:1629–1640.

Table S2. ϕ29 phages and plasmids used

Phage	Source or reference
ϕ29 wild-type	Laboratory stock
sus14(1242)	(1)
sus2*(*513)	(2)
sus3*(*91)	(2)

Plasmid	Relevant features	Reference
pSG1729	*bla amyE3′ spc* P_{xyl}*-gfpmut1′ amyE5′*, N-terminal GFP fusion vector	(3)
pSG5472	pSG1729 derivative containing *yfpmut2* gene instead of *gfpmut1*	(4)
pDP150-CFP/TP8-PRD1	pDP150-CFP-2 containing *cfp*::*VIII* PRD1 fusion	This work
pSGDM3	pSG5472 containing *yfp*::p2 fusion	(4)
pSGDM5	pSG5472 containing *yfp*::p3 fusion	This work
pDR200	Vector containing *cfp (Bs)* optimized for *B. subtilis* expression	(5)
pDP150	pDR111 derivative *thrC* integrating vector containing $P_{hyper\text{-}spank}$	(6)
pDP150-CFP	pDP150 containing *cfp (Bs)*	This work
pDP150-CFP-2	pDP150-CFP containing a *SpeI* site at the MCS	This work
pDP150-CFP/TP	pDP150-CFP-2 containing *cfp*::*p3* fusion	This work
pDP150-CFP/TP-Nt	pDP150-CFP-2 containing *cfp*::*p3-Nt* fusion	This work
pDP150-CFP/TP-NtI	pDP150-CFP-2 containing *cfp*::*p3-NtI* fusion	This work
pDP150-CFP/TP-I	pDP150-CFP-2 containing *cfp*::*p3-I* fusion	This work
pDP150-CFP/TP-ΔNt	pDP150-CFP-2 containing *cfp*::*p3-δNt* fusion	This work
pDP150-CFP/TP-Ct	pDP150-CFP-2 containing *cfp*::*p3-Ct* fusion	This work
pDP150-TP	pDP150 containing ϕ29 *gene 3*	This work
pET-28b(+)	*E. coli* expression vector for protein purification	Novagen
pT7-3	*E. coli* expression vector for protein purification	(7)
pT7-3-TP	pT7-3 vector containing gene *3*	8)
pET-TP/Nt	pET-28b(+) containing *gene 3-Nt* region	This work
pET-TP/NtI	pET-28b(+) containing *gene 3-NtI* region	(8)
pET-TP/ΔNt	pET-28b(+) containing *gene 3-ICt* region	(8)
pET-TP/Ct	pET-28b(+) containing *gene 3-Ct* region	(8)

1. Jiménez F, Camacho A, De La Torre J, Viñuela E, Salas M (1977) Assembly of *Bacillus subtilis* phage ϕ29. 2. Mutants in the cistrons coding for the non-structural proteins. *Eur J Biochem* 73:57–72.
2. Moreno F, Camacho A, Viñuela E, Salas M (1974) Suppressor-sensitive mutants and genetic map of *Bacillus subtilis* bacteriophage ϕ29. *Virology* 62:1–16.
3. Lewis PJ, Marston AL (1999) GFP vectors for controlled expression and dual labelling of protein fusions in *Bacillus subtilis*. *Gene* 227:101–110.
4. Muñoz-Espín D, et al. (2009) The actin-like MreB cytoskeleton organizes viral DNA replication in bacteria. *Proc Natl Acad Sci USA* 106:13347–13352.
5. Doan T, Marquis KA, Rudner DZ (2005) Subcellular localization of a sporulation membrane protein is achieved through a network of interactions along and across the septum. *Mol Microbiol* 55:1767–1781.
6. Kearns DB, Losick R (2005) Cell population heterogeneity during growth of *Bacillus subtilis*. *Genes Dev* 19:3083–3094.
7. Tabor S, Richardson CC (1985) A bacteriophage T7 RNA polymerase/promoter system for controlled exclusive expression of specific genes. *Proc Natl Acad Sci USA* 82:1074–1078.
8. Pérez-Arnaiz P, et al. (2007) Involvement of phage ϕ29 DNA polymerase and terminal protein subdomains in conferring specificity during initiation of protein-primed DNA replication. *Nucleic Acids Res* 35:7061–7073.

Table S3. Oligonucleotides used

Oligonucleotide	Sequence
YFP-TP_U	5′-gat aac tcg aga tgg cga gaa gtc cac gta tac gc-3′
YFP-TP_L	5′-ttt aag aat tcc tag aac ccc ttt aag ctt aga tca aag tc-3′
CFP(BS)_U	5′-cgt gat taa aag ctt aca taa gga gga ac-3′
CFP(BS)_L	5′-tta agg agc tag cct tat aaa gtt cgt cca tgc caa gtg taa tgc-3′
150-SpeI-1	5′-gca agc taa ttc ggt gga aac tag ttc atc att tcc ttc cga aaa aac gg-3′
150-SpeI-2	5′-ccg ttt ttt cgg aag gaa atg atg aac tag ttt cca ccg aat tag ctt gc-3′
TP_1	5′-cat gcg cta gcg aaa gga gat aa cgc aac atg gcg aga ag-3′
TP_2	5′-ttt aag cat gcc tag aac ccc ttt aag ctt aga tc-3′
TP_U	5′-gag atg cat gca cat ggc gag aag tcc acg tat-3′
TP_L	5′-ttt aaa cta gtc tag aac ccc ttt aag ctt a-3′
TP-Nt_L	5′-ttt tca cta gtt tat cac ata tta gca cgg tta gtg aaa gag g-3′
TP-NtI_L	5′-ttc tta cta gtt tac taa ggg tct gtt ctc atc tcc atg c-3′
TP-I_U	5′-taa ccg cat gca tat gcg tta tca gtt cga aaa g-3′
TP-Ct_U	5′-gag aag cat gcc tca gta tta tga aaa gaa aat gat aca g-3′
TP-NcoI_U	5′-taa cgc acc atg gcg aga agt cca cgt ata cgc att aag g-3′
TP-NtI-NotI_L	5′-ctt ttc agc ggc cgc agg gtc tgt tct cat ctc cat gct t-3′
TP-NdeI_U	5′-aac gcc ata tgg cga gaa gtc cac gta tac-3′
TP-Nt-NotI_L	5′-tct ttg cgg ccg ctt atc aca tat tag cac ggt tag tga aaa gag g-3′
TP-I-NdeI_U	5′-cgg cag cca tat gcg tta tca gtt cg-3′
TP-BamHI_L	5′-cgc ggg atc cgg agc cta gaa cc-3′
TP-Ct-NdeI_U	5′-gcg cgc ata tgt att atg aaa aga aaa tg-3′
yshC_U	5′-ccg cgg atc cca tca ttt tac ggg-3′
yshC_L	5′-ggg tcg aca ctt cct gtc cgc ttt cac g-3′
R-OUT-SUPER	5′-aaa tag att ttc ttt ctt ggc tac-3′
R-25	5′-aaa gta ggg tac agc gac aac ata c-3′
TP8-R	5′-cgg aag gca tgc tca tgg cga aga aaa aac cag tag aa-3′
TP8-L	5′-acg gcg act agt tca tta aac ccc ctt gct gcc ata gcc gcg-3′